Inferring Light-cycle-oil Stream Properties Using Soft Sensors

J. Joucowski[a], P. M. Ndiaye[b], M. L. Corazza[b], and M. K. Lenzi[b,*]

[a]Refinaria Presidente Getúlio Vargas – REPAR / PETROBRAS.
Rodovia do Xisto (BR-476), Km 16 – Araucária, 83700–970, PR, Brazil

[b]Department of Chemical Engineering, Federal University of Paraná (UFPR), Polytechnic Center (DTQ/ST/UFPR), Jardim das Américas, Curitiba, 81531–980, PR, Brazil

Original scientific paper
Received: September 27, 2012
Accepted: March 1, 2013

The intensive necessity of hydrotreatment units for diesel production is pushing petroleum companies to seek alternatives to frame the produced streams into ultra low sulphur diesel (ULSD) specifications. One of the main difficulties in ULSD production is the presence of compounds from dibenzothiophenes (DBT), which are of difficult hydrotreatment. The LCO cutpoint control represents an interesting alternative to overcome this situation. Thus, the objective of this work was to develop a soft sensor using linear models and neural networks considering a set of historical data of temperature, pressure and flow obtained from industrial plant information. Lab and process data concerning a period of 18 months was successfully used to infer 10%, 30%, 50%, 70% and 90% ASTM D-86 recovery temperature. Based on correlation matrix plots, using lab data as the dependent variable and plant data as independent variable, different models were developed for LCO cutpoint prediction. For all models, correlation coefficient between model predictions and experimental data were above 0.95.

Key words:
Inference, soft sensor, diesel, property, neural network

Introduction

The use of hydrotreating processes for meeting products specification in an oil refinery is now mandatory due to environmental constraints required. Diesel and gasoline, products which had relatively loose specifications some decades ago, nowadays have narrow ranges of production, especially related to sulfur content, distillation and combustion properties, such as cetane number for diesel and octane number for gasoline.[1]

Regarding low sulfur content diesel production, a deep hydrodesulphurization process is recommended. It is usually accomplished by the reaction of a diesel stream and hydrogen in a fixed bed reactor operating at suitable temperature and pressure conditions.[2] During this process, many hydrogenation reactions involving the existing heteroatom in the feed (as sulfur, nitrogen and oxygen, besides aromatic ring opening and hydrocracking) may occur. The extension of each reaction depends on the process severity, and along the reaction period an increase in water, hydrogen sulphide and ammonia concentrations in the gas stream with hydrogen partial pressure reduction, caused by the hydrogen consumption due to these reactions is expected.[3] Generally, light cycle oil (LCO) streams arising from fluid catalytic cracking (FCC) units are more difficult to treat not only due the high nitrogen and sulfur content, but also due to high aromaticity. Regarding sulfur-based components, the presence of compounds from the benzothiophenes, particularly the dimethyldibenzothiophenes (DMDBT) and superior, plays a key role on downstream processing and product quality.[4]

Nowadays, industry has been making use of different methodologies, such as hydrogen partial pressure increase, addition of extra reactors and catalyst, reactor temperature rising and catalyst change.[5–6] However, the implementation of these changes in existing hydrotreating units, besides the usual high costs, could also be of difficult implementation due to space and time constraints.[7] In order to enable a faster and cheaper production of ULSD, an alternative approach relies on performing a feed control, relieving the necessity of the deep desulphurization of refractory species by just rejecting this species to other streams. Moreover, distillation endpoint controlling also helps to remove some nitrogen species as acridine that compete with the same catalyst sites used in the hydrodesulphurization.[8]

Aimed at proper operation, a control loop requires adequate instrumentation. On the other hand, this may not exist or may have prohibitive costs. Therefore, the use of virtual sensors or soft sensors becomes an attractive approach. Some advantages are the low cost

*Corresponding author: Prof. Marcelo K. Lenzi – email:lenzi@ufpr.br – phone: + 55 41 3361 3587

of implementation and parallel operation with on-line analyzers for creating monitoring systems.[9] This type of sensor can be either based on fundamental principles[10–11] or on empirical equations.[12] Although extrapolation is not recommended when using an empirical-based soft sensor, its simplicity, easy maintenance and fast implementation makes it very attractive, especially for industrial applications.[8]

Literature reports some applications on the development and use of soft sensor in petroleum processing. For example, Bolf et al.[13] reported the development of a soft sensor for diesel fuel quality estimation using neural networks. The authors also reported[14] the development of soft sensors for kerosene properties estimation and control in crude distillation unit. Fortuna et al.[15] described the use of soft analyzers for a sulfur recovery unit and Zhou et al.[16] presented the inferential estimation of kerosene dry point in refineries with varying crudes. Rogina et al.[17] developed a soft sensor for continuous estimation of light naphtha vapor pressure. Chatterjee and Saraf[18] reported a tool for on-line estimation of product properties for crude distillation units, focusing on the true boiling point (TBP) curve prediction. Carroll et al[19] reported an improved prediction of hydrocarbon flash points from boiling point data by using empirical correlations. Zendehboudi et al[20] presented the use of an artificial neural network to adequately predict the condensate-to-gas ratio for retrograde gas condensate reservoirs.

In this sense, this work reports the development of soft sensor for inferring the properties of LCO of an industrial oil refining unit, using both linear correlation models and neural networks. More specifically, the inference of 10%, 30%, 50%, 70% and 90 % ASTM D-86 recovery temperature was focused.

Soft sensor development

Industrial unit

A schematic diagram of the unit used in this study is shown in Fig. 1. It comprises an industrial distillation column, which receives the product from the reactor (riser/separator drum) and performs the initial separation from the cuts for treatment or improvement in further processing units.

The subsystem of interest is highlighted in Fig. 1 and represents a sidecut where LCO stream is produced in the unit. In this process plant, this stream has two different purposes: it can be either used as diluent for feed oil or it can be hydrotreated

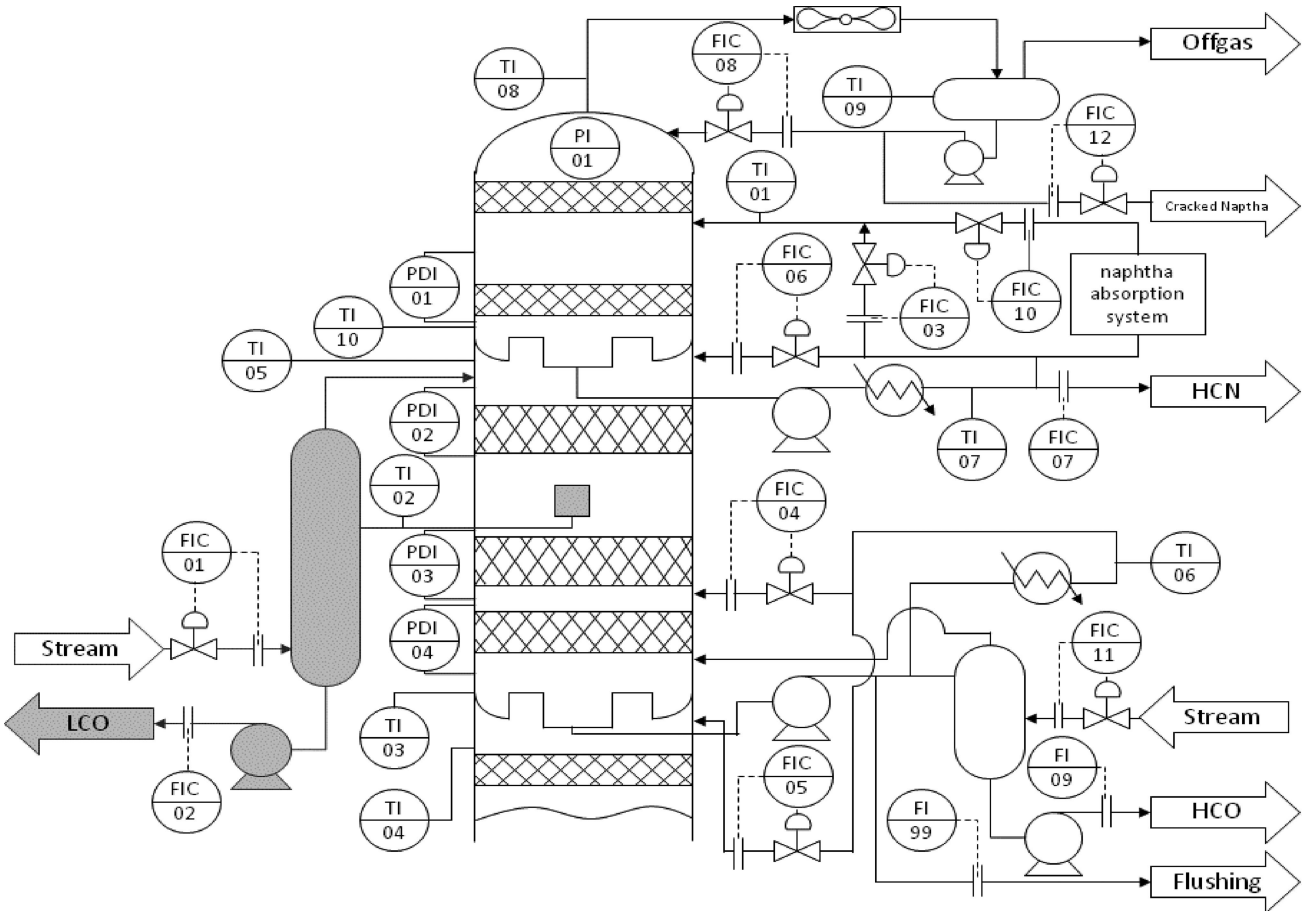

Fig. 1 – *FCC Distillation Column P&ID*

for blending in order to obtain diesel. As the price difference between these two products is too high, the operation to transform LCO into diesel is mostly often chosen, since the final requirements are fully accomplished by the hydrotreaters.

Variable selection and data handling

An 18 month operating horizon was selected to obtain the experimental data set used in this work. Process data regarding flow, temperature and pressure were obtained from plant information software and the experimental ASTM D-86 curve data resulted from lab activities. Before using, process and lab data were checked for consistency. More specifically, only steady state operating conditions (flow, temperature and pressure) were selected together with the respective lab analysis. During process data evaluation, a steady state operation was considered to exist in a set if, for flow and pressure measurements a standard deviation lower than 5% could be achieved together with a temperature standard deviation lower than 1ºC.The values of 5% and 1ºC were obtained from PETROBRAS internal standard procedures, based on process expert knowledge.[21]

Model structuring and selection of regression parameters

In order to develop accurate soft sensors, two different approaches were considered: linear in the parameters correlations[19] and MLP (Multi Layer Perceptron) neural networks.[22] Concerning the linear correlations, the following models were evaluated, after preliminary analysis of the data sets correlation and tendencies.

$$TX\%_{Corr01} = a_0 + a_1 \cdot (TI\text{-}02) + a_2 \cdot (FFI\text{-}01) \quad (1)$$

$$TX\%_{Corr02} = a_0 + a_1 \cdot (TI\text{-}02) + a_2 \cdot (FFI\text{-}01) + a_3 \cdot (PY\text{-}01) \quad (2)$$

$$TX\%_{Corr03} = a_0 + a_1 \cdot (TY\text{-}01) + a_2 \cdot (FFI\text{-}01) \quad (3)$$

$$TX\%_{Corr04} = a_0 + a_1 \cdot (TY\text{-}01) \quad (4)$$

$$TX\%_{Corr05} = a_0 + a_1 \cdot (TI\text{-}03) + a_2 \cdot (TI\text{-}05) + a_3 \cdot (FIC\text{-}04) + a_4 \cdot (FIC\text{-}06) + a_5 \cdot (PY\text{-}01) + a_6 \cdot (TY\text{-}01) + a_7 \cdot (FFI\text{-}01) + a_9 \cdot (FFI\text{-}02) \quad (5)$$

$$TX\%_{Corr06} = a_0 + a_1 \cdot (TI\text{-}02) + a_2 \cdot (FFI\text{-}01) + \Sigma(Ti\% \cdot a_i) \quad (6)$$

$$TX\%_{Corr07} = a_0 + a_1 \cdot (TY\text{-}01) + a_2 \cdot (FFI\text{-}01) + \Sigma(Ti\% \cdot a_i) \quad (7)$$

where a_j are the estimated parameters; $TX\%_{Corr(i)}$ is the i^{th} correlation studied to predict the X% of the ASTM D-86 distillation points (X = 10;30; 50; 70; 90); the other variables were directly extracted from plant data, according to Fig. 1.

It can be observed that Eq. (6) and Eq. (7) can be considered somehow hybrid models as they use not only independent process data (TY-01, FFI-01 and TI-02), but also experimental lab results (Ti%). Some variables considered for model development, which are not shown in Fig. 1, were calculated using the equations given in Table 1. It is important to state that variable TY-01 (LCO Withdraw Corrected Temperature) was obtained with the Clausius-Clay-

Table 1 – *Calculated variables*

TAG	Description	Calculation blocks
FY-02	Reactor Stream Sum	= ([FIC-18] + [FIC-19] + [FIC-20] + [FIC-21] + [FI-22] + [FIC-23] + + [FIC-24] + [FIC-25] + [FIC-26] + [FY-01]) · 1000 kg · ton^{-1}
FY-03	Rectification Stream Sum	= ([FIC-01] + [FIC-11] + [FIC-18]) · 1000 kg · ton^{-1}
FY-04	Stream Molar Flow	= ([FY-02) + [FY-03)]) / 18 kg kmol^{-1}
FY-05	Offgas Molar Flow	= ([FI-15]) / 22.73 Nm³ kmol^{-1}
FY-06	LPG Molar Flow	= ([FI-16] x $d_{20/4\_LPG}$) / (MW_{LPG} x 24 h · d^{-1})
FY-07	Cracked Naphtha Molar Flow	= ([FIC-17] x $d_{20/4\_Naphtha}$) / ($MW_{Naphtha}$ x 24 h · d^{-1})
FY-08	HCN Molar Flow	= ([FIC-07] x $d_{20/4\_HCN}$) / (MW_{HCN})
FY-09	LCO Molar Flow	= ([FIC-07] x $d_{20/4\_LCO}$) / (MW_{LCO})
FY-10	LCO Molar Fraction	= ([FY-10]) / ([FY-04] + [FY-05] + [FY-06] + [FY-07] + [FY-08] + [FY-09])
PY-01	LCO Sidecut Pressure [kgf/cm² / mm H_2O]	= [PI-01] + ([PDI-01] + [PDI-02]) · 0.0001
TY-01	LCO Withdraw Corrected Temperature	
FFI-01	LCO Volumetric Yield	= [FIC-02] / ([FI-13] + [FIC-14])
FFI-02	Reflux Ratio	= [FIC-08] / [FIC-12]

$d_{20/4\_i}$ standard density of the cut at 20 °C reference of each cut; M_{w_i} molar weight of each cut; $\Delta Hvap_{LCO}$ heat of vaporization of LCO (kJ kmol^{-1}); P_{ref} reference pressure (kPa); R universal gas constant.

Table 2 – *Average Cut Properties*

Cut	Density at 20 °C (kg m^{-3})	Molecular Weight (kg $kmol^{-1}$)
LPG	546.0	49.6
Cracked Naphtha	757.5	98.4
HCN	906.8	180
LCO	965.3	199.3

peron equation.[19,23] All the average properties used in this work are presented in Table 2, which were obtained using historical data from the plant and other lab analyzes.

The parameter estimation problem used Eq.(8) as the objective function and the optimization problem was solved by standard methods previously reported.[24] Models were statistically evaluated by considering simultaneously the lowest value of the objective function, the highest value of the correlation coefficient, the lowest number of parameters and, mainly, the lowest values of parametric variance.

In the scenario using neural networks, feedforward architecture, using MLP networks were considered. An extensive work was performed on the selection of input variables of the neural networks, by considering different number and also different types of variables, similarly to the linear correlation models (see Eq. (1) to Eq. (7)). The unitary input, which represents the bias from the neuron, was also included during training/testing steps.

For each network, the following parameters were evaluated: i) number of internal neurons; ii) the type activation function in the hidden and in the output layer (logistic, exponential, hyperbolic and identity); iii) the percentage of the data set considered for training and testing purposes. In all cases, training algorithm was BFGS (since networks did not have a large number of neurons[22]), with a weight decay set with a minimal value of 0.001 and maximum value of 0.01 for both layers (hidden and output). After studying all different combinations of neural networks, the best one for each percentage of the ASTM-86 curve was chosen considering lowest prediction error and smallest neuron number achieved during training / testing procedures.

Results and discussion

All the linear models previously presented (see. Eq.(1) to Eq.(6)) were used for predicting 10%, 30%, 50%, 70% and 90% recovery temperature. Table 3 presents only the best model for each of the recovery temperatures, based on the value of the correlation coefficient (r), value of the objective function (F_{OBJ} – see Eq.(7)) and the parametric variance. All models were tested for all recovery temperatures. It can be observed that for 10% to 50% the linear models were capable of correlate the lab data to process measurements, presenting correlation coefficients over 0.95. For all estimated parameters, the respective standard deviation was lower than the parameter value itself, indicating a statistical significance. For 70% and especially for 90% recovery temperature the linear model parameter presented an unsatisfactory correlation, even with using other distillation points. These results reflect that, as higher gets the boiling point, more specific components (heavier components) exist in that cut, and because of that, worst linear correlations will be obtained. Experimental normalized (0 for lowest value and 1 for highest) data against normalized model predictions are shown in Fig. 2. It can be observed that for 10% to 50% model predictions are within the confidence range of 95%, showing that simple models can be successfully used as soft sensors. Regarding 70% and 90% the linear correlation models performance is not as good as for the previous cases. Although the model predictions lie within the confidence region, due to the lower correlation coefficient and larger parametric variance, this region is larger, consequently, a larger spread of the plotted points is expected, reducing the soft sensor accuracy. Besides, it can also be observed that even the simpler correlations, i.e., having few parame-

Table 3 – *Parameter estimation summary for linear models*

Best model		$T10\%_{Corr01} = a_0 + a_1 \times (TI\text{-}02) + a_2 \times (FFI\text{-}01)$		
$a_0 =$	0.51	$sa_0 =$	0.06	$r = 0.9688$
$a_1 =$	0.54	$sa_1 =$	0.05	$F_{OBJ} = 412.3614$
$a_2 =$	–0.48	$sa_2 =$	0.06	
Best model		$T30\%_{Corr01} = a_0 + a_1 \times (TI\text{-}02) + a_2 \times (FFI\text{-}01)$		
$a_0 =$	0.54	$sa_0 =$	0.05	$r = 0.9648$
$a_1 =$	0.48	$sa_1 =$	0.05	$F_{OBJ} = 363.8474$
$a_2 =$	–0.46	$sa_2 =$	0.05	
Best model		$T50\%_{Corr04} = a_0 + a_1 \times (TY\text{-}01)$		
$a_0 =$	0.11	$sa_0 =$	0.02	$r = 0.9565$
$a_1 =$	0.83	$sa_1 =$	0.04	$F_{OBJ} = 590.5986$
Best model		$T70\%_{Corr04} = a_0 + a_1 \times (TY\text{-}01)$		
$a_0 =$	0.13	$sa_0 =$	0.03	$r = 0.8226$
$a_1 =$	0.57	$sa_1 =$	0.05	$F_{OBJ} = 115.0751$
Best model		$T90\%_{Corr06} = a_0 + a_1 \times (T10\%) + a_2 \times (T50\%) + a_3 \times (TI\text{-}02) + a_4 \times (FFI\text{-}01)$		
$a_0 =$	0.02	$sa_0 =$	0.12	$r = 0.8125$
$a_1 =$	-1.3	$sa_1 =$	0.2	$F_{OBJ} = 247.7183$
$a_2 =$	1.8	$sa_2 =$	0.2	
$a_3 =$	0.13	$sa_3 =$	0.1	
$a_4 =$	0.27	$sa_4 =$	0.1	

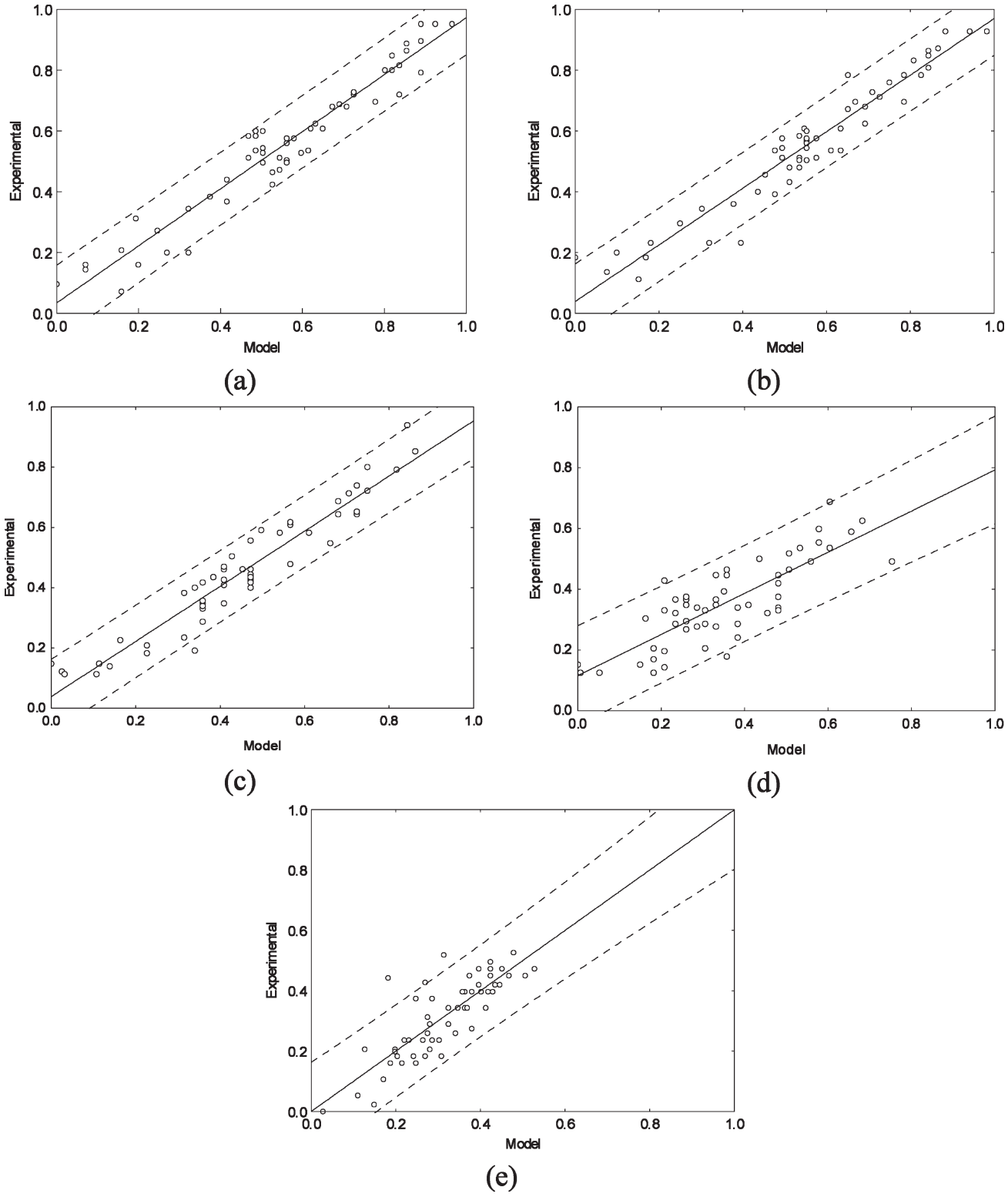

Fig. 2 – *Linear models (a) 10%; (b) 30%; (c) 50%; (d) 70%; (e) 90%*

ters, led to satisfactory results. This is an important feature as although empirical, the correlations can have some physical meaning, for example, when temperature (or compensated temperature) rises, the temperature of that cut also rises, and when LCO yield increases, the cut point falls because more heavy cracked naphtha goes inside the column to LCO withdraw.

Regarding neural networks models, different combinations of inputs, based on process expert knowledge, were tested. Each test considered not only different percentages of training/testing data

Table 4 – *Inputs leading to the best neural network*

T10%	T30%	T50%	T70%	T90%
TI-03	TI-01	TI-01	10%	10%
TI-05	TI-06	TI-06	50%	50%
FIC-04	TI-07	TI-07	TI-02	TI-03
FIC-06	TI-09	TI-09	FFI-01	TI-05
PY-01	FIC-03	FIC-03	Bias	FIC-04
TY-01	FIC-04	FIC-04		FIC-06
FFI-01	FIC-05	FIC-05		PY-01
FFI-02	FIC-06	FIC-06		TY-01
Bias	FIC-10	FIC-10		FFI-01
	PY-01	PY-01		FFI-02
	FFI-02	FFI-02		Bias
	Bias	Bias		

(50/50, 70/30, 90/10), but also different activation functions. Table 4 reports the set of input variables of the best neural networks obtained for each ASTM D-86 percentage. Due to the neural network features, a larger number of inputs are necessary when compared to the linear models.

Table 5 presents a summary of the neural networks performance. It can also be noted that the hidden layer did not require a large number of neurons, probably because of the experimental data correlation shown by the linear models. A careful analysis shows that the neural network prediction performance concerning the lower percentages was worse than the performance for 70% and 90%. This can also be observed from Fig. 3. Comparing Fig. 2 to Fig. 3, for lower percentages, 10%; 30%; 50% the linear correlation models not only led to better performances, but also are simpler models, which can be easily updated by proper parameter re-estimation. On the other hand, for 70% and 90% provided a superior performance, comparing Fig. 2d to Fig. 3d and Fig. 3d to Fig. 3e, respectively. It can be seen that the neural network predictions are closer to the experimental as the points in Fig. 3d and Fig. 3e are closer to the straight line that indicates that a good correlation coefficient as indicated in Table 5. This happened due to the intrinsic nature of the neural network, which was able to handle possible nonlinear correlation features of the experimental data. Finally, it is important to mention that for all neural networks, the best training/testing percentage was 70/30.

Conclusions

LCO cutpoint control represents an interesting alternative for ULSD production, providing a way to avoid LCO degradation to fuel oil and profitability losses. However, for an appropriate control loop performance, a reliable sensor is necessary. Towards this, soft sensors can play a key role. In this work, two different approaches were used to develop soft sensors to predict LCO ASTM D-86 curve of industrial oil refining equipment. In the first approach, linear correlations were developed and after parameter estimation, 10%; 30% and 50% of the curve were successfully inferred by comparison with lab data. For higher percentages, such as 70% and 90%, linear models did not present the same performance. Towards this, neural networks were used as an alternative approach for the sensor development. Using different inputs, neural networks could be successfully trained and used for adequate prediction of 70% and 90% of the ASTM D-86 curve. For all models, correlation coefficients between model predictions and experimental data were above 0.95. Based on the obtained results, the applied methodologies could be effectively applied as soft sensors for monitoring LCO cutpoint and reducing refractory species in this stream.

ACKNOWLEDGEMENTS

The authors thank CNPq and Fundação Araucária (Brazilian Agencies) for scholarships and PETROBRAS S/A for data supplying and access to plant facilities.

Table 5 – *Summary of Network Results*

Cut D-86	Architecture	Performance correlation coefficient		Error		Activation Function	
		training	test	training	test	hidden layer	exit
10	8–4–1	0.96000	0.97282	0.00251	0.00119	Exponential	Identity
30	11–4–1	0.96160	0.96263	0.00231	0.00331	Tanh	Tanh
50	11–4–1	0.94043	0.97250	0.00320	0.00390	Tanh	Tanh
70	4–3–1	0.98172	0.99078	0.00077	0.00042	Tanh	Tanh
90	10–4–1	0.97660	0.90655	0.00082	0.00298	Tanh	Identity

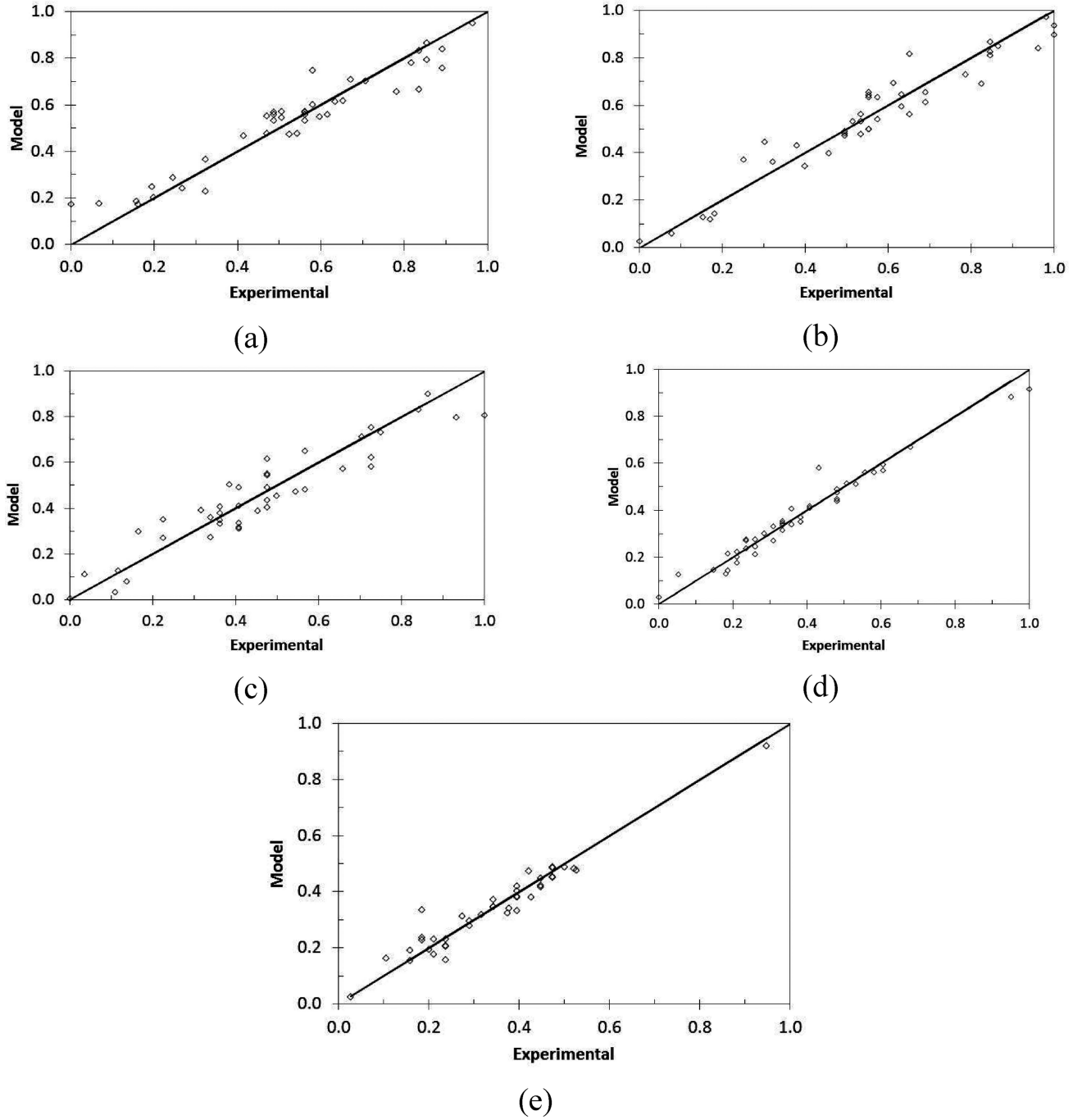

Fig. 3 – *Neural network (a) 10%; (b) 30%; (c) 50%; (d) 70%; (e) 90%*

References

1. *Peng, C., Huang, X., Liu, T.,Zeng, R., Liu, J., Guan, M.,* Hydrocarb. Process. **91** (2012) 65.
2. *Ganguly, S.K.,* Pet. Sci. Technol. **30** (2012) 1187.
3. *Navarrete, C., Garcia, R., Sepulveda, C., Gil-Llambias, F.J., Fierro, J.L.G., Escalona, N.,* Catal. Lett. **141** (2011) 1796.
4. *Song, C., Ma, X.L.,* Appl. Catal., B **41** (2003) 207.
5. *Zhang, Y.L., Yang, Y.X., Han, H.X., Yang, M., Wang, L., Zhang, Y.N., Jiang, Z.X., Li, C.,* Appl. Catal., B **119** (2012) 13.
6. *Srivastava, V.C,* RSC Adv. **2** (2012) 759.
7. *Gary, J.H.,Handwerk, G.E.,* Petroleum Refining: Technology and Economics, Marcel Dekker, New York, 2001.
8. *Fortuna, L., Graziani, S., Rizzo, A. ,Xibilia, M. G.,* Soft Sensors for Monitoring and Control of Industrial Processes, Springer, London, 2006.
9. *Goel, S., Shah, J.,* Hydrocarb. Process. **84** (2005) 81.
10. *Friedman, Y.Z., Schuler, M.,* Hydrocarb. Process. **82** (2003) 43.
11. *Friedman, Y.Z., Neto, E.A., Porfirio, C.R.,* Hydrocarb. Process. **81** (2002) 53.
12. *Fortuna, L., Graziani, S., Xibilia, M.G.,* IEEE Instru. Meas. Mag. **8** (2005) 26.

13. *Bolf, N.,Galinec, G.,Baksa, T.,* Chem. Eng. Technol. **33** (2010)405.
14. *Bolf, N.,Galinec, G.,Ivandic, M.,* Chem. Biochem. Eng. Q. **23** (2009) 277.
15. *Fortuna, L., Rizzo, A., Sinatra, M.,Xibilia, M.G.,* Control Eng. Pract. **11** (2003) 1491.
16. *Zhou, C, Liu, QY, Huang, DX, Zhang, J.,* J. Process Control **22** (2012) 1122.
17. *Rogina, A.,Sisko, I.,Mohler, I.,Ujevic, Z.,Bolf, N.,* Chem. Eng. Res. Des. **89** (2011) 2070.
18. *Chatterjee, T., Saraf, D.N.,* J. Process Control **14** (2004) 61.
19. *Carroll, F.A., Lin, C.Y.,Quina, F.H.,* Energ. Fuel. **24** (2010) 4854.
20. *Zendehboudi, S.,Ahmadi, M.A., James, L.,Chatzis, I.,* Energ. Fuel. **26** (2012) 3432.
21. *Lima, D.F.B., Zanella, F.A., Teixeira, A.C., Luz, L.F.L., Gontarski, C.A.U., Gomes, E.M., Chiquitto, S.H., Lenzi, M.K.,* Development of Multivariate Statistical-Based Tools for Monitoring of Sour Water Unit. In deBritoAlves, RM; doNascimento, CAO; Biscaia, EC (Editors) Computer-Aided Chemical Engineering, Vol 27, pp. 1479–1484, Elsevier, Netherlands, 2009.
22. *Haykin, S.,* Neural Networks: A Comprehensive Foundation, Prentice Hall, Upper Saddle River, 1998.
23. *Sandler, S.I.,*Chemical, Biochemical, and Engineering Thermodynamics, John Wiley & Sons, New York, 2006.
24. *Isfer, L.A.D., Lenzi, M.K., Lenzi, E.K.,* Lat. Am. Appl. Res. **40** (2010) 193.